



Yang, Z., Jiang, B., McNamara, M. E., Kearns, S. L., Pittman, M., Kaye, T. G., Orr, P. J., Xu, X., & Benton, M. J. (2019). Pterosaur integumentary structures with complex feather-like branching. *Nature Ecology and Evolution*, 3(1), 24-30. <https://doi.org/10.1038/s41559-018-0728-7>

Peer reviewed version

License (if available):
Other

Link to published version (if available):
[10.1038/s41559-018-0728-7](https://doi.org/10.1038/s41559-018-0728-7)

[Link to publication record in Explore Bristol Research](#)
PDF-document

This is the accepted author manuscript (AAM). The final published version (version of record) is available online via Springer Nature at <https://doi.org/10.1038/s41559-018-0728-7> . Please refer to any applicable terms of use of the publisher.

University of Bristol - Explore Bristol Research

General rights

This document is made available in accordance with publisher policies. Please cite only the published version using the reference above. Full terms of use are available:
<http://www.bristol.ac.uk/red/research-policy/pure/user-guides/ebr-terms/>

Pterosaur integumentary structures with complex feather-like branching

Zixiao Yang¹, Baoyu Jiang¹, Maria E. McNamara², Stuart L. Kearns³, Michael Pittman⁴, Thomas G. Kaye⁵, Patrick J. Orr⁶, Xing Xu⁷, Michael J. Benton³

1. Center for Research and Education on Biological Evolution and Environments,
School of Earth Sciences and Engineering, Nanjing University, Nanjing 210023,
China

2. School of Biological, Earth and Environmental Sciences, University College Cork,
Cork T23 TK30, Ireland

3. Department of Earth Sciences, University of Bristol, Bristol BS8 1RJ, UK

4. Vertebrate Palaeontology Laboratory, Department of Earth Sciences, University of
Hong Kong, Pokfulam, Hong Kong, China

5. Foundation for Scientific Advancement, Sierra Vista, Arizona USA

6. UCD School of Earth Sciences, University College Dublin, Belfield, Dublin 4
D04V1W8, Ireland

7. Key Laboratory of Vertebrate Evolution and Human Origins, Institute of Vertebrate
Paleontology and Paleoanthropology, Chinese Academy of Sciences, Beijing 100044,
China

Pterosaurs were the first vertebrates to achieve true flapping flight, but in the absence of living representatives, many questions concerning their biology and lifestyle remain unresolved. Pycnofibres, the integumentary coverings of pterosaurs, are particularly enigmatic: although many reconstructions depict fur-like coverings composed of pycnofibres, their affinities and function are not fully understood. Here we report the preservation in two anurognathid pterosaur specimens of morphologically diverse pycnofibres that show diagnostic features of feathers, including non-vaned grouped filaments and bilaterally branched filaments, hitherto considered unique to maniraptoran dinosaurs, and preserved melanosomes with diverse geometries. These findings could imply that feathers had deep evolutionary origins in ancestral archosaurs, or that these structures arose independently in pterosaurs. The presence of feather-like structures suggests that anurognathids, and potentially other pterosaurs, possessed a dense filamentous covering that likely functioned in thermoregulation, tactile sensing, signalling, and aerodynamics.

Feathers are the most complex integumentary appendages in vertebrates¹. Most feathers in modern birds possess an axial shaft from which branch lateral barbs and barbules. Much is known about the anatomy, developmental biology, and genomic regulation of these structures, but their deep evolutionary origin is controversial^{2–4}. Feathers and feather-like integumentary structures have been reported in many theropod dinosaurs (including birds)^{3,5} and ornithischians such as *Psittacosaurus*⁶, *Tianyulong*⁷, and *Kulindadromeus*⁸. Feather-like or hair-like structures, termed pycnofibres⁹, have also been reported in several pterosaur specimens^{9–13}, but their nature is not resolved.

Here we report remarkably well-preserved pycnofibres in two anurognathid pterosaurs and demonstrate, using evidence from morphology, chemistry and macroevolutionary analyses, that the preserved pycnofibres bear key features of feathers: monofilaments, two types of non-vaned grouped filaments, bilaterally branched filaments that were previously considered unique to maniraptoran dinosaurs, and preserved melanosomes with diverse geometries. Both specimens studied are from the Middle–Late Jurassic Yanliao Biota (ca. 165–160 Mya¹⁴). NJU–57003 (Nanjing University) is a newly excavated specimen from the Mutoudeng locality and CAGS–Z070 (Institute of Geology, Chinese Academy of Geological Sciences), which has been noted briefly for its feather-like branched pycnofibres¹³, is from the Daohugou locality. Both specimens are near-complete and well-articulated, with extensive soft tissues (Figs. 1 and 2, and Supplementary Figs. 1–5). Both specimens are identified as anurognathids¹⁷ (see Supplementary text for osteological descriptions).

Preserved soft tissues include structural fibres (actinofibrils) and pycnofibres. Structural fibres, common in the pterosaur wing membrane^{9,12,18}, are observed only in the posterior portion of the uropatagium in CAGS–Z070 (Fig. 1o–p). As reported elsewhere, they are parallel to subparallel and closely packed. Individual fibres are 0.08–0.11 mm wide (ca. 5 fibres per mm) and at least 1.9 mm long. Pycnofibres are preserved extensively in both pterosaur specimens (especially CAGS–Z070; Figs. 1

and 2, and Supplementary Figs. 1, 4 and 5) and are discriminated from structural fibres based on their curved morphology and overlapping arrangement. In the posterior portion of the uropatagium in CAGS-Z070, pycnofibres co-occur with structural fibres; oblique intersections reflect superposition of these features during decay (Fig. 1o–p).

Pycnofibres are categorized here into four types. Type 1 occurs around the head, neck, shoulder, torso, all four limbs and tail of both specimens (Figs. 1c–e, o–p, 2b–c and f). It comprises curved monofilaments that are 3.5–12.8 mm long and 70–430 μm wide. Some short, distally tapering examples discriminate between dark-toned lateral margins and light-toned axial regions, especially near the filament base where the light-toned axis is wider, suggesting a tube-like morphology (Fig. 1c–e). Type 2 is preserved in the neck, proximal forelimb, plantar metatarsus and proximal tail regions of CAGS-Z070. It consists of bundles of curved filaments of similar length that appear to form brush-like structures at the distal ends of thicker filaments (2.0–13.8 mm long and 80–180 μm wide) (Fig. 1f–h). The latter may represent individual thick filaments or fused proximal regions of thinner distal filaments. Type 3 occurs around the head of CAGS-Z070. It comprises straight to slightly curved, distally tapered, central filaments (4.5–7.0 mm long and 50–450 μm wide) with short lateral branches that diverge from the central filament near the midpoint (Fig. 1i–k). There are five Type 3 filaments identified on the head, next to five similar filaments likely of the same nature but obscured by overlapping filaments (Supplementary Fig. 5b). Type 4 occurs on the wing membrane of both specimens. It comprises tufts of curved filaments (2.5–8.0 mm long and 70–130 μm wide) that diverge proximally (Figs. 1l–n and 2d–e), in contrast to the clear separation between Type 1 filaments (Fig. 1o–p).

Filamentous integumentary structures in extant and fossil vertebrates commonly contain melanin-bearing organelles (melanosomes). Scanning electron microscopy (SEM) of the filamentous structures of NJU-57003 reveals densely packed microbodies $0.70 \pm 0.11 \mu\text{m}$ long and $0.32 \pm 0.05 \mu\text{m}$ wide (Fig. 2g–h, Supplementary Figs. 4a–f, 6 and 7, and Supplementary Table 2). As with most melanosome-rich fossil feathers^{19–21}, energy dispersive X-ray spectroscopy (EDS) spectra of the filaments are dominated by a major peak for carbon (Supplementary Fig. 8). These carbonaceous microbodies resemble fossil melanosomes in terms of their geometry, dense packing, parallel alignment relative to the long axis of the integumentary structure (i.e. barbules in Paraves), and preservation within the matrix of the filament (see Supplementary text). Most of the microbodies are oblate and morphologically similar to those that are usually interpreted as phaeomelanosomes in fossils¹⁹ (Fig. 2h). Rod-shaped examples, usually interpreted as eumelanosomes in fossils¹⁹ (Fig. 2g), are rare.

Fourier transform infrared spectroscopy (FTIR) of samples of pterosaur filaments shows four major peaks unique to the filaments (Fig. 2i). These peaks are consistent with the absorption regions of amide I at ca. 1650 cm^{-1} (principally the C=O asymmetric stretching vibration with some C–N bending), amide II at ca. 1540 cm^{-1} (a combination of N–H in-plane bending and C–N and C–C stretching as in indole and pyrrole in melanin and amino acids), and aliphatic C–H stretching at 2850 cm^{-1}

and 2918 cm^{-1} ²². These peaks also occur in spectra obtained from extant feathers^{21,23}, fossil feathers of the paravian *Anchiornis*²⁰, and melanosomes isolated from human hair²⁴. Further, spectra of the pterosaur filaments more closely resemble those of pheomelanin-rich red human hair in the stronger absorption regions at ca. 2850 cm^{-1} and 2918 cm^{-1} and higher resolution in the region ca. 1500–1700 cm^{-1} than those from eumelanin-rich black human hair and the ink sac of cuttlefish²⁴. This, together with the SEM results, suggests that the densely packed microbodies in the pterosaur filaments are preserved melanosomes. The amide I peak at 1650 cm^{-1} is more consistent with α -keratin (characteristic of extant mammal hair²⁵) than β -keratin (the primary keratin in extant avian feathers^{22,26}). This signal may be original or diagenetic; the molecular configuration of keratin²⁶ and other proteins²⁷ can alter under mechanical stress and changes in hydration levels.

The ultrastructural and chemical features of the pterosaur filaments confirm that they are hair-like or feather-like integumentary structures. The four types of filaments described here show distinct distributions and morphologies. They are separated clearly from the sedimentary matrix by sharp boundaries (Supplementary Fig. 4g–i). There is no evidence that one or more filament type(s) were generated taphonomically, e.g. through selective degradation or fossilization, or superimposition of filaments. For instance, although Type 1 and 4 filaments occur widely in both specimens, Type 4 occurs only in the wings, while Type 1 occupies the remaining body regions. Type 1 filaments are thus not degraded products of Type 4, and Type 4 filaments do not represent superimposed clusters of Type 1 filaments. Filament types 2 and 3 occur only in CAGS–Z070. Type 3 occurs only in the facial area and is associated with Type 1, where Types 2 and 4 are not evident. Type 3 filaments are thus not degraded Type 2 or 4 filaments. Central filaments of Type 3 are morphologically identical to the short, distally tapering filaments of Type 1, but the branching filaments are much thinner ($< 40 \mu\text{m}$ (Type 3) versus $> 70 \mu\text{m}$ (Type 1) wide) and shorter ($< 0.6 \text{ mm}$ vs. $> 3.5 \text{ mm}$ long) than the latter. The branching filaments are thus unlikely to reflect superimposition of clusters of Type 1 filaments. In contrast, the distal ends of Type 2 filaments are similar, and have a similar distribution pattern to, Type 1 filaments. An alternative interpretation, that Type 2 filaments might represent superimposition of Type 1 filaments at their proximal ends, is unlikely (see detailed discussion in Supplementary text). Feathers and feather-like integumentary structures have been reported in non-avian dinosaurs, although debate continues about their true nature². These structures have been ascribed to several morphotypes, some absent in living birds^{3,5}, and provide a basis to analyse the evolutionary significance of pterosaur pycnofibres. The pterosaur Type 1 filaments resemble monofilaments in the ornithischian dinosaurs *Tianyulong* and *Psittacosaurus* and the coelurosaur *Beipiaosaurus*: unbranched, cylindrical structures with a midline groove that widens towards the base (presumed in *Beipiaosaurus*)^{3,5}. The pterosaur Type 2 filaments resemble the brush-like bundles of filaments in the coelurosaurs *Epidexipteryx* and *Yi*^{3,5,28}: both comprise parallel filaments that unite proximally. The morphology and circum-cranial distribution of pterosaur Type 3 filaments resemble bristles in modern birds¹, but surprisingly do not correspond to any reported

morphotype in non-avian dinosaurs. The Type 3 filaments recall bilaterally branched filaments in *Sinornithosaurus*, *Anchiornis*, and *Dilong*, but the latter filaments branch throughout their length rather than halfway along the central filament(s), as in the pterosaur structure^{3,5}. The pterosaur Type 4 filaments are identical to the radially branched, downy feather-like morphotype found widely in coelurosaurs such as *Sinornithosaurus*, *Beipiaosaurus*, *Protarchaeopteryx*, *Caudipteryx*, and *Dilong*^{3,5}.

The filamentous integumentary structures in our anurognathid pterosaurs are thus remarkably similar to feathers and feather-like structures in non-avian dinosaurs. Intriguingly, cylindrical (Type 1), radially symmetrical branched (Types 2 and 4) and bilaterally symmetrical branched (Type 3) filaments clearly coexisted in individual animals; these structures may represent transitional forms in the evolution of feathers, as revealed by developmental studies^{3,5}. These new findings warrant revision of the origin of complex feather-like branching integumentary structures from Dinosauria to Avemetatarsalia, the wider clade that includes dinosaurs, pterosaurs, and close relatives^{4,29}. The early evolutionary history of bird feathers and homologous structures in dinosaurs, and the multiple complex pycnofibres of pterosaurs, is enigmatic. A previous study concluded that the common ancestor of these clades bore scales and not filamentous integumentary appendages², but this result emerged only when the filaments of pterosaurs were coded as non-homologous with those of dinosaurs. There are no morphological criteria, however, for such a determination. The presence of multiple pycnofibre types and their morphological, ultrastructural and chemical similarity to feathers and feather-like structures in various dinosaurian clades, confirms their likely homology with filamentous structures in non-avian dinosaurs and birds. Comparative phylogenetic analysis produces equivocal results: maximum likelihood modelling of plausible ancestral states, against various combinations of branch length and character transition models (Supplementary text and Supplementary Fig. 9, Table 3), reveals various potential solutions. The statistically most likely result (Fig. 3 and Supplementary Table 3, highest log-likelihood value) shows that the avemetatarsalian ancestors of dinosaurs and pterosaurs possessed integumentary filaments, with highest likelihood of possessing monofilaments; tufts of filaments, and, especially, brush-type filaments, are less likely ancestral states. This confirms that feather-like structures arose in the Early or Middle Triassic. The alternative tree for Dinosauria, with Ornithischia and Theropoda paired as Ornithoscelida³⁰, produces an identical result.

We present these modelling data with caution, however, for two reasons: (1) the tree rooting method can influence the result (Supplementary Table 3), favouring results in which either scales are the basal condition or where non-theropod feather-like structures and feathers evolved independently (Supplementary Figure 9, Table 3), and (2) there is no adequate way to model probabilities of evolution of all six feather types, or to model probabilities of transitions between the six different feather types.

The discovery of multiple types of feather-like structures in pterosaurs has broad implications for our understanding of pterosaur biology and the functional origin of feather-like structures in Avemetatarsalia^{31,32}. Potential functions of these structures include insulation, tactile sensing, streamlining and coloration (primarily for

camouflage and signalling), as for bristles, down feathers and mammalian hairs³¹⁻³⁴. Type 1, 2 and 4 filaments could shape a filamentous covering around the body and wings (Fig. 4) that might have functioned in streamlining the body surface in order to reduce drag during flight, as for modern bat fur or avian covert feathers^{33,35}. Type 1 and 2 filaments occur in considerably high densities, particularly around the neck, shoulder, hindlimb and tail regions where the high degree of superposition prevents easy discrimination of adjacent fibres. This, along with the wide distribution and frayed appearance, resembles mammalian underfur adapted for thermal insulation^{36,35}. Despite the less dense packing of Type 4 filaments on the wings, the morphology of the structures is consistent with a thermoregulatory function: down feathers can achieve similar insulation as mammalian hair with only about half the mass, due to their air-trapping properties and high mechanical resilience, effective in retaining an insulating layer of still air³⁸. This may optimize the encumbrance of the large wing area to wing locomotion¹⁸. Type 3 filaments around the jaw (Fig. 4) may have had tactile functions in e.g. prey handling, information gathering during flight, navigating in nest cavities and on the ground at night, similar to bristles in birds³⁹.

Methods

Sampling. The specimen NJU-57003 is represented by two fragmented slabs, both containing original bone, fossilized soft tissues, and natural moulds of bones. Each slab was glued together along the fissures by fossil dealers with the fossil on the surfaces untouched. The specimen CAGS-Z070 is represented by a single unbroken slab. Small flakes (1–3 mm wide) of samples with preserved integument and/or enclosing sediments were carefully removed from the inferred integumentary filaments from different parts of NJU-57003 (Supplementary Figs. 1a and 4a–c) using a dissecting scalpel. This method was used to avoid sampling from degraded products of other tissues, such as dermis, epidermis, or even internal organs. Most samples were not treated further; the remainder were sputter-coated with Au to enhance SEM resolution (Fig. 2g–h and Supplementary Figs. 4a–f and 6). All experiments described below were repeated in order to validate the results.

SEM. Samples were examined using a JEOL 8530F Hyperprobe at the School of Earth Sciences, University of Bristol, and a LEO 1530VP scanning electron microscope at the Technical Services Centre, Nanjing Institute of Geology and Palaeontology, Chinese Academy of Sciences. Both instruments were equipped with a secondary electron (SE) detector, a back-scattered electron (BSE) detector and an energy dispersive X-ray spectrometer (EDS).

Measurements of melanosomes. The geometry of melanosomes was measured from SEM images using the image-processing program ImageJ (available for download at <http://rsbweb.nih.gov/ij/>). We measured maximum short and long axis length of melanosomes that were oriented perpendicular to line of sight, and from these data we calculated mean and coefficient of variation (CV) of the long and short axis, and mean aspect ratio (long:short axis). Based on the proposed taphonomic alteration of fossil

melanosome size (shrinkage up to ~20% in both length and diameter)^{40,41}, we modelled potential diagenetic alteration by enlarging original measurements by 20%.

FTIR microspectroscopy. Samples of the filamentous tissues and the associated sediments were removed separately from NJU-57003 and placed on a BaF₂ plate without further treatment. The IR absorbance spectra were collected using a Thermo iN10MX infrared microscope with a cooled MCT detector, at the School of Earth Sciences, University of Bristol. The microscope was operated in transmission mode with a 15x15 micron aperture. 10 spectra were obtained from the filamentous tissues. The spectra show consistent results and the example presented in Fig. 2 shows the highest signal to noise ratio and was obtained with 2 cm⁻¹ resolution and 2000 scans.

Fluorescence microscopy. Selected areas with extensive soft tissue preservation in NJU-57003 were investigated and photographed using a Zeiss Axio Imager Z2 microscope with a digital camera (AxioCam HRc) and a fluorescence illuminator (514 nm LED) attached, at the Technical Services Centre, Nanjing Institute of Geology and Palaeontology, Chinese Academy of Sciences.

Laser-stimulated fluorescence (LSF) imaging and data reduction protocol. LSF images were collected using the protocol of Kaye et al.^{15,16}. NJU-57003 was imaged with a 405 nm 500 mw laser that was projected into a vertical line by a Laserline Optics Canada lens. The laser line was swept repeatedly over the specimen during the exposure time for each image in a dark room. Images were captured with a Nikon D610 DSLR camera fitted with an appropriate long pass blocking filter in front of the lens to prevent image saturation by the laser. Standard laser safety protocols were followed during laser usage. The images were post processed in Photoshop CS6 for sharpness, colour balance and saturation.

Phylogenetic macroevolutionary analysis. In order to analyse the evolution of feather characters, data were compiled on known integumentary characters across dinosaurs and pterosaurs. The basic data were taken from the Supplementary data of Barrett et al.², comprising 74 dinosaurs (33 ornithischians, seven sauropods and 44 theropods (including four Mesozoic birds)); to this dataset we added four pterosaurs. Barrett et al.² scored taxa for three integumentary states (scales, filaments, feathers) in their macroevolutionary analyses. We checked and followed these basic categories and added three more; we then cross-referenced these six categories against the feather morphotypes defined by Xu et al.⁴². The categories used herein are: scales (1; not included in Xu et al.⁴²), monofilaments (2; morphotypes 1 and 2 in Xu et al.⁴²), brush-like filaments associated with a planar basal feature (3; morphotypes 4 and 6 in Xu et al.⁴²), tufts of filaments joined basally (4; morphotype 3 in Xu et al.⁴²), open pennaceous vane, lacking secondary branching (5; morphotype 5 in Xu et al.,⁴²), and closed pennaceous feathers comprising a rachis-like structure associated with lateral branches (barbs and barbules) (6). There was some uncertainty over feathers coded herein as type 3, which could correspond to morphotype 6, or morphotypes 4 and 6 in

Xu et al.⁴². However, the only taxa coded with these as the most derived feather type are *Sordes pilosus* and *Beipiaosaurus inexpectus*. These taxa belong to separate clades and thus the calculation of ancestral states is not affected by how our feather type 3 is coded (i.e. whether treating morphotypes 4 and 6 of Xu et al.⁴² in combination or separately).

As in previous studies², we used maximum-likelihood (ML) approaches to explore trait evolution. There are many methods to estimate ancestral states for continuous characters, but choices are more limited for discrete characters, such as here, where only ML estimation of ancestral states is appropriate⁴³. We calculated ML reconstructions of ancestral character states using the ‘ace’ function of the ape R package⁴⁴, with tree branch lengths estimated in terms of time, derived using the ‘timePaleoPhy’ function in the paleotree package⁴⁵ and the ‘DatePhylo’ function in the strap R package⁴⁶. These enabled us to assess results according to three methods of estimating branch lengths, the ‘basic’ method, which makes each internal node in a tree the age of its oldest descendant, the ‘equal branch length’ (equal) method, which adds a pre-determined branch length (often 1 Myr) to the tree root and then evenly distributes zero-length branches at the base of the tree, and the ‘minimum branch length’ (mbl) method, which minimizes inferred branching times and closely resembles the raw, time-calibrated tree. A problem with the ‘basic’ branch length estimation is that it results in many branch lengths of length zero, in cases where many related taxa are of the same age; in these cases, we added a line of code to make such zero branch lengths equal to 1/1000000 of the total tree length. A criticism of the mbl method is that it tends to extend terminal branching events back in time, especially when internal ghost lineages are extensive², but this is not the case here, and the base of the tree barely extends to the Triassic / Jurassic boundary.

We ran our analyses using three evolutionary models with different rates of transition between the specified number of character states (six here), namely “ER”, an equal-rates model, “ARD”, an all-rates-different model and “SYM”, a symmetrical model. These were calculated using the ‘ace’ function in ape² and the ‘add.simmap.legend’ function of the R package ‘phytools’⁴⁷.

In a further series of analyses, we attempted to model the macroevolution of all traits, as coded (see Supplementary results), so coding multiple trait values for taxa that preserve multiple feather types. This did not shed much light on patterns of evolution of feather types because the multiple trait codings (e.g. 1,2 or 2,5,6) were each made into a new state, making 14 in all, and these were not linked. Therefore, the six multiply coded taxa that each had feather type 6 were represented as six independent states and their evolution tracked in those terms. Further, we attempted to separate the six characters, so they would track through the tree, whether recorded as singles or multiples in different taxa; however, we did not have the information to enable us to do this with confidence because of gaps in coding. In terms of reality, these multiply coded taxa still represent an incomplete sample of the true presence and absence of character states - by chance, many coelurosaurs are not coded for scales (1) or monofilaments (1), and yet it is likely they all had these epidermal appendages. Therefore, attempting to run such multiple codings, with characters

either as groups or coded independently, encounters so many gaps that the result is hard to interpret. Our approach is to code the most derived feather in each taxon, and that too is incomplete because of fossilization gaps, but at least it represents a minimal, or conservative, approach to trait coding and hence to the discoveries of macroevolutionary patterns of feather evolution; complete fossil data might show wider distributions of each feather type and hence deeper hypothesized points of origin. Complete coding of feather types would of course allow each trait to be tracked in a multiple-traits analysis.

Data availability

The data that support the findings of this study are available from the corresponding authors upon reasonable request.

References

- 1 Lucas, A. M. S. & Peter, R. *Avian anatomy: integument* (U.S. Agricultural Research Service, Washington, 1972).
- 2 Barrett, P. M., Evans, D. C. & Campione, N. E. Evolution of dinosaur epidermal structures. *Biol. Lett.* **11**, 20150229 (2015).
- 3 Xu, X. *et al.* An integrative approach to understanding bird origins. *Science* **346**, 1253293 (2014).
- 4 Di-Poï, N. & Milinkovitch, M. C. The anatomical placode in reptile scale morphogenesis indicates shared ancestry among skin appendages in amniotes. *Sci. Adv.* **2**, e1600708 (2016).
- 5 Chen, C. F. *et al.* Development, regeneration, and evolution of feathers. *Ann. Rev. Anim. Biosci.* **3**, 169–195 (2015).
- 6 Mayr, G., Pittman, M., Saitta, E., Kaye, T. G. & Vinther, J. Structure and homology of *Psittacosaurus* tail bristles. *Palaeontol.* **59**, 793–802 (2016).
- 7 Zheng, X. T., You, H. L., Xu, X. & Dong, Z. M. An Early Cretaceous heterodontosaurid dinosaur with filamentous integumentary structures. *Nature* **458**, 333–336 (2009).
- 8 Godefroit, P. *et al.* A Jurassic ornithischian dinosaur from Siberia with both feathers and scales. *Science* **345**, 451–455 (2014).
- 9 Kellner, A. W. *et al.* The soft tissue of *Jeholopterus* (Pterosauria, Anurognathidae, Batrachognathinae) and the structure of the pterosaur wing membrane. *Proc. Biol. Sci.* **277**, 321–329 (2010).
- 10 Sharov, A. G. New flying reptiles from the Mesozoic of Kazakhstan and Kirgizia (in Russian). *Akad. nauk SSSR Paleont. Inst. Tr.* **130**, 104–113 (1971).
- 11 Czerkas, S. A. & Ji, Q. A new rhamphorhynchoid with a headcrest and complex integumentary structures. In: S. J. CZERKAS (Ed), Feathered dinosaurs and the origin of flight (Blanding, The Dinosaur Museum), 15–41 (2002).
- 12 Unwin, D. M. & Bakhurina, N. N. *Sordes pilosus* and the nature of the pterosaur flight apparatus. *Nature* **371**, 62–64 (1994).
- 13 Ji, Q. & Yuan, C. Discovery of two kinds of protofeathered pterosaurs in the Mesozoic Daohugou Biota in the Ningcheng region and its stratigraphic and

- biologic significances. *Geol. Rev.* **48**, 221–224 (2002).
- 14 Xu, X., Zhou, Z., Sullivan, C., Wang, Y. & Ren, D. An updated review of the Middle-Late Jurassic Yanliao Biota: chronology, taphonomy, paleontology and paleoecology. *Acta Geol. Sin. (Engl. Ed.)* **90**, 2229–2243 (2016).
 - 15 Wang, X. *et al.* Basal paravian functional anatomy illuminated by high-detail body outline. *Nat. Commun.* **8**, (2017).
 - 16 Kaye, T. G. *et al.* Laser-stimulated fluorescence in paleontology. *PloS one* **10**, e0125923 (2015).
 - 17 Unwin, D. M. On the phylogeny and evolutionary history of pterosaurs. *Geol. Soc., London, Spec. Publ.* **217**, 139–190 (2003).
 - 18 Frey, E., Tischlinger, H., Buchy, M. C., & Martill, D. M. New specimens of Pterosauria (Reptilia) with soft parts with implications for pterosaurian anatomy and locomotion. *Geol. Soc., London, Spec. Publ.* **217**, 233–266 (2003).
 - 19 Lindgren, J. *et al.* Interpreting melanin-based coloration through deep time: a critical review. *Proc. R. Soc. B* **282**, 20150614 (2015).
 - 20 Lindgren, J. *et al.* Molecular composition and ultrastructure of Jurassic paravian feathers. *Sci. Rep.* **5**, 13520 (2015).
 - 21 Barden, H. E. *et al.* Morphological and geochemical evidence of eumelanin preservation in the feathers of the Early Cretaceous bird, *Gansus yumenensis*. *PLoS One* **6**, e25494 (2011).
 - 22 Bendit, E. Infrared absorption spectrum of keratin. I. Spectra of α -, β -, and supercontracted keratin. *Biopolymers* **4**, 539–559 (1966).
 - 23 Martinez-Hernandez, A. L., Velasco-Santos, C., De Icaza, M. & Castano, V. M. Microstructural characterisation of keratin fibres from chicken feathers. *Int. J. Envir. Pollut.* **23**, 162–178 (2005).
 - 24 Liu, Y. *et al.* Comparison of structural and chemical properties of black and red human hair melanosomes. *Photochem. Photobiol.* **81**, 135–144 (2005).
 - 25 Alibardi, L. Adaptation to the land: the skin of reptiles in comparison to that of amphibians and endotherm amniotes. *J. Exp. Zool.* **298B**, 12–41 (2009).
 - 26 Kreplak, L., Doucet, J., Dumas, P. & Briki, F. New aspects of the α -helix to β -sheet transition in stretched hard α -keratin fibers. *Biophys. J.* **87**, 640–647 (2004).
 - 27 Yassine, W., Taib, N., Federman, S., Milochau, A., Castano, S., Sbi, W. Manigand, C., Laguerre, M., Desbat, B., Oda, R. & Lang, J. Reversible transition between α -helix and β -sheet conformation of a transmembrane domain. *Biochim. Biophys. Acta – Biomembranes.* **1788**, 1722–1730 (2009).
 - 28 Xu, X. *et al.* A bizarre Jurassic maniraptoran theropod with preserved evidence of membranous wings. *Nature* **521**, 70–73 (2015).
 - 29 Donoghue, P. C. J. & Benton, M. J. Rocks and clocks: calibrating the Tree of Life using fossils and molecules. *Trends Ecol. Evol.* **22**, 424–431 (2007).
 - 30 Baron, M. G., Norman, D. B. & Barrett, P. M. A new hypothesis of dinosaur relationships and early dinosaur evolution. *Nature* **543**, 501–506 (2017).
 - 31 Persons IV, W. S. & Currie, P. J. Bristles before down: a new perspective on the functional origin of feathers. *Evolution* **69**, 857–862 (2015).
 - 32 Ruxton, G. D., Persons IV, W. S. & Currie, P. J. A continued role for signaling

- functions in the early evolution of feathers. *Evolution* **71**, 797–799 (2017).
- 33 Bullen, R. D. & McKenzie, N. L. The pelage of bats (Chiroptera) and the presence of aerodynamic riblets: the effect on aerodynamic cleanliness. *Zoology* **111**, 279–286 (2008).
- 34 Caro, T. The adaptive significance of coloration in mammals. *BioScience* **55**, 125–136 (2005).
- 35 Homberger, D. G., & de Silva, K. N. Functional microanatomy of the feather-bearing integument: implications for the evolution of birds and avian flight. *Amer. Zool.* **40**, 553–574 (2000).
- 36 Scholander, P., Walters, V., Hock, R. & Irving, L. Body insulation of some arctic and tropical mammals and birds. *Biol. Bull.* **99**, 225–236 (1950).
- 37 Ling, J. K. Pelage and molting in wild mammals with special reference to aquatic forms. *Quart. Rev. Biol.* **45**, 16–54 (1970).
- 38 Gao, J., Yu, W. & Pan, N. Structures and properties of the goose down as a material for thermal insulation. *Text. Res. J.* **77**, 617–626 (2007).
- 39 Cunningham, S. J., Alley, M. R., & Castro, I. Facial bristle feather histology and morphology in New Zealand birds: implications for function. *J. Morphol.* **272**, 118–128 (2011).
- 40 McNamara, M. E., Briggs, D. E. G., Orr, P. J., Field, D. J. & Wang, Z. Experimental maturation of feathers: implications for reconstructions of fossil feather colour. *Biol. Lett.* **9**, 20130184 (2013).
- 41 Colleary C, Dolocan A, Gardner J, *et al.* Chemical, experimental, and morphological evidence for diagenetically altered melanin in exceptionally preserved fossils. *Proc. Natl. Acad. Sci.* **112**, 12592–12597 (2015).
- 42 Xu, X., Zheng, X. & You, H. Exceptional dinosaur fossils show ontogenetic development of early feathers. *Nature* **464**, 1338–1341 (2010).
- 43 Pagel, M. Detecting correlated evolution on phylogenies: a general method for the comparative analysis of discrete characters. *Proc. R. Soc. Lond. B* **255**, 37–45 (1994).
- 44 Paradis, E. *Analysis of Phylogenetics and Evolution with R*. (Springer Science & Business Media, 2011).
- 45 Bapst, D. W. paleotree: paleontological and phylogenetic analyses of evolution. v. 2.3. See <https://github.com/dwbapst/paleotree> (2015).
- 46 Bell, M. A. & Lloyd, G. T. Strap: an R package for plotting phylogenies against stratigraphy and assessing their stratigraphic congruence. *Palaeontol.* **58**, 379–389 (2015).
- 47 Revell, L. J. phytools: an R package for phylogenetic comparative biology (and other things). *Methods Ecol. Evol.* **3**, 217–223 (2012).

Supplementary Information is available in the online version of the paper.

Acknowledgements

We thank Qiang Ji, Shu'an Ji and Hao Huang for access to the specimen CAGS–Z070, as well as Simon C. Kohn, Yan Fang, Chunzhao Wang and Tong He for

laboratory assistance. This work was supported by the National Natural Science Foundation of China (41672010; 41688103) and the Strategic Priority Research Program (B) of the Chinese Academy of Sciences (XDB26000000) to B.Y.J., the Research Grant Council of Hong Kong-General Research Fund (17103315) to M.P., ERC-StG-2014-637691-ANICOLEVO to M.E.M., and Natural Environment Research Council Standard Grant NE/1027630/1 to M.J.B.

Author Contributions

B.Y.J. and M.J.B. designed the research, Z.X.Y., B.Y.J. and X.X. systematically studied the specimens, Z.X.Y., S.L.K., M.E.M, and P.J.O. did the SEM analysis, Z.X.Y. and B.Y.J. did the FTIR analysis, M.P. and T.G.K. did the LSF imaging, data reduction and interpretation, M.J.B. did the maximum likelihood analyses, and Z.X.Y., B.Y.J., M.J.B., M.E.M, X.X. and P.J.O. wrote the paper; all authors approved the final draft of the paper.

Author Information

Reprints and permissions information is available at www.nature.com/reprints. The authors declare no competing financial interests. Correspondence and requests for materials should be addressed to B.Y.J. (byjiang@nju.edu.cn) or M.J.B. (mike.benton@bristol.ac.uk).

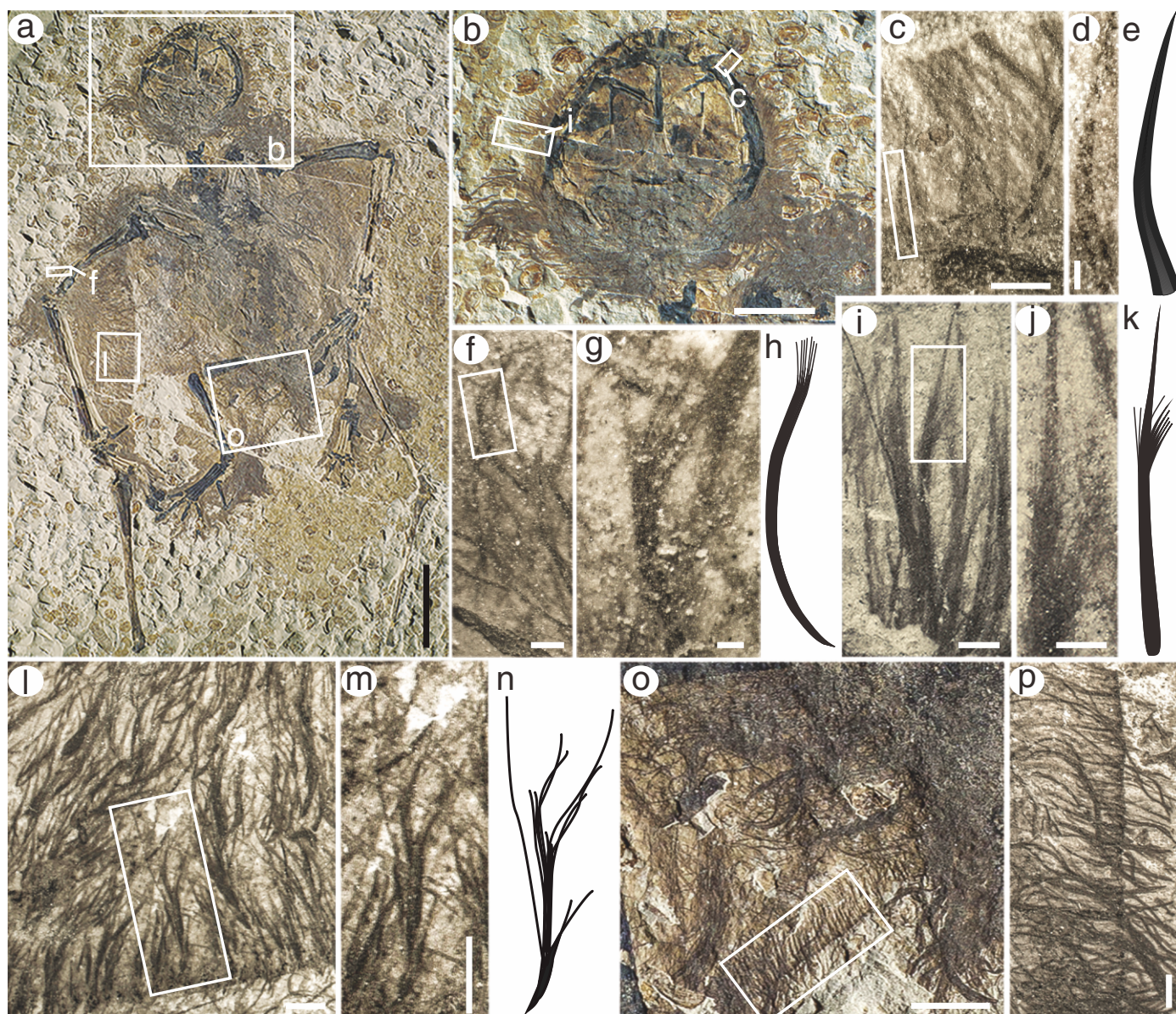
Figure 1 | Integumentary filamentous structures in CAGS–Z070. **a**, Overview shows extensive preservation of soft tissues. **b–p**, Details of the integumentary filaments in the regions indicated in **a** on the head and neck (**b–d**, **i–j**), forelimb (**f–g**), wing (**l–m**) and tail (**o–p**), and illustrated reconstructions of the filaments (**e**: Type 1 filament; **h**: Type 2 filament; **k**: Type 3 filament; **n**: Type 4 filament). Scale bars: 20 mm in **a**; 10 mm in **b**; 500 μ m in **c** and **i**; 100 μ m in **d**; 1 mm in **f**, **l**, **m** and **p**; 200 μ m in **g** and **j**; 5 mm in **o**.

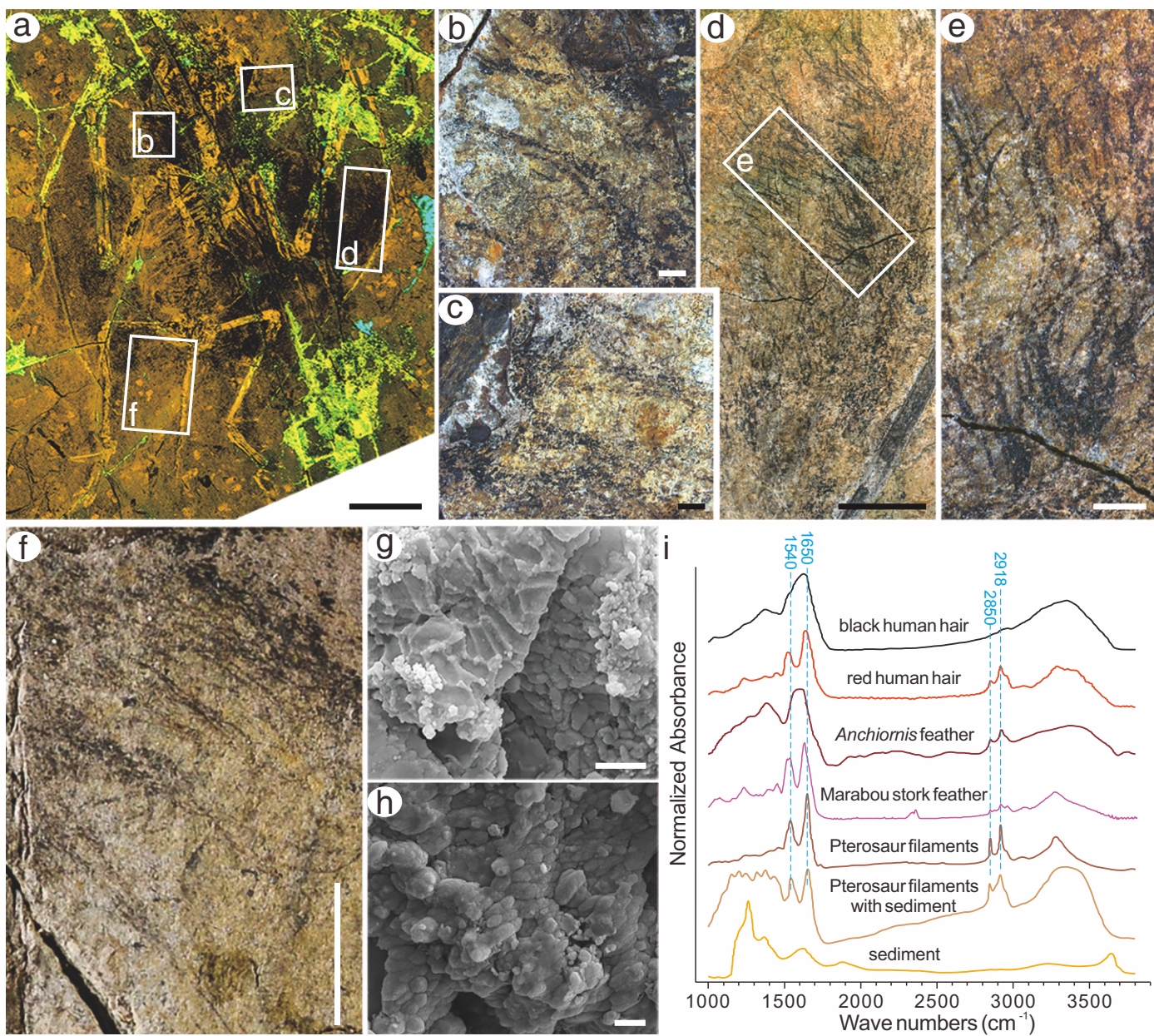
Figure 2 | Preservation, microstructure and chemistry of the integumentary filamentous structures in NJU–57003. **a**, Laser-stimulated fluorescence^{6,15,16} image highlights extensive preservation of soft tissues (black areas). **b–f**, Details of the integumentary filaments in the regions indicated in **a** on the head and neck (**b–c**), wing (**d–e**) and tail (**f**). **g–h**, Scanning electron micrographs of the monofilaments on the neck and hindlimb of NJU–57003 (samples 10 and 39, respectively, Supplementary Fig. 1a) show densely packed, elongate and oblate melanosomes. **i**, FTIR absorbance spectra of the monofilaments, monofilaments with sediment matrix, and sediment matrix in NJU–57003 (Sample 15, Supplementary Fig. 1a) compared with spectra from a feather of *Anchiornis* (from ref. ²⁰), extant Marabou stork feather (from ref. ²¹) and black and red human hair melanosomes (from ref. ²⁴). Scale bars: 20 mm in **a**; 1 mm in **b**, **c** and **e**; 5 mm in **d** and **f**; 1 μ m in **g** and **h**.

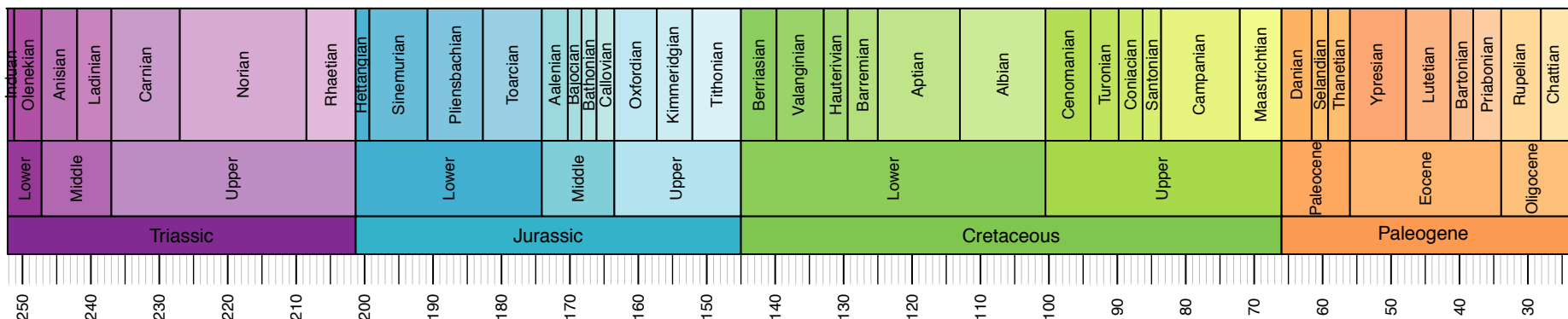
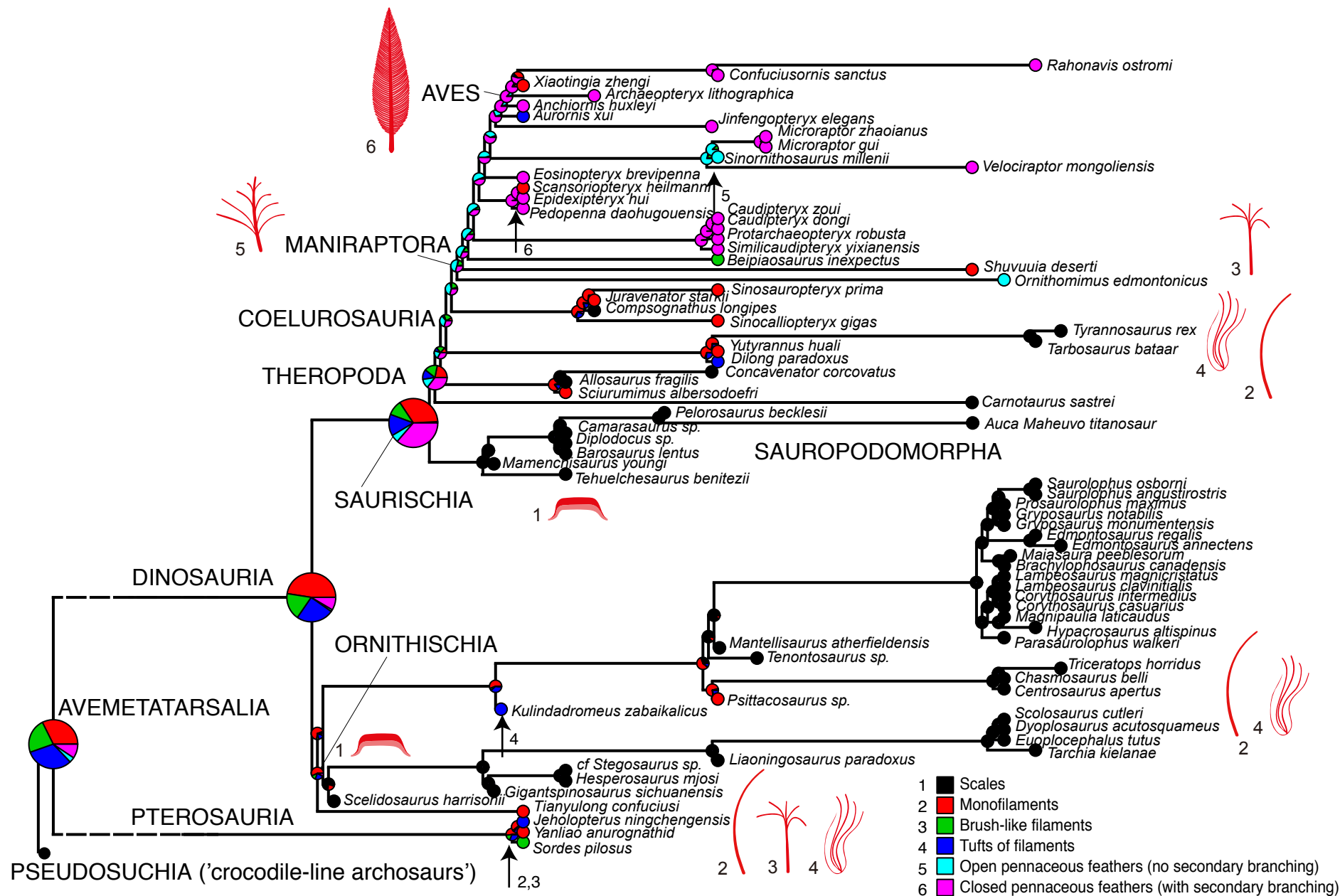
Figure 3 | Phylogenetic comparative analysis of integumentary filament and feather evolution in pterosaurs and archosaurs. The phylogeny is scaled to

geological time, with recorded terminal character states for each species, and estimated ancestral character states at the lower nodes. The model is the most likely of the maximum likelihood models, based on minimum-branch lengths (mbl) and transitions occurring as all-rates-different (ARD), but other results with lower likelihoods show scales as ancestral. The ancestral state reconstruction shows a combination of monofilaments, tuft-like filaments, and brush-type filaments as the ancestral state for Avemetatarsalia and for Dinosauria. The estimated ancestral state for Theropoda comprises all five feather states. Numbered small vertical arrows indicate earliest occurrences of feather types 2–6. Two hypotheses for timing of avian feather origins are indicated: A, early origin, at the base of Avemetatarsalia in the Early Triassic, or B, late origin, at the base of Maniraptora in the Early–Middle Jurassic.

Figure 4 | Reconstruction of one of the studied anurognathid pterosaurs, exhibiting diverse types of pycnofibres distributed in different body parts.







A early origin of feathers

B late origin of feathers